In vitro transformation of primary human hepatocytes: Epigenetic changes and stemness properties

Floriane Pez, Patricia Gifu, Davide Degli-Esposti, Nadim Fares, Anaïs Lopez, Lydie Lefrançois, Maud Michelet, Michel Rivoire, Brigitte Bancel, Bakary S. Sylla, et al.

In vitro transformation of primary human hepatocytes: epigenetic changes and stemness properties

Floriane PEZ[a], Patricia GIFU[a], Davide DEGLI ESPOSTI[b], Nadim FARES[a], Anaïs LOPEZ[a], Lydie LEFRANCOIS[a], Maud MICHELET[a], Michel RIVOIRE[c], Brigitte BANCEL[a,d], Bakary S. SYLLA[e], Zdenko HERCEG[b], Philippe MERLE[a,f,†], Claude CARON de FROMENTEL[a,†,*]

[a] INSERM U1052, CNRS 5286, Univ Lyon, Université Claude Bernard Lyon 1, Centre Léon Bérard, Centre de Recherche en Cancérologie de Lyon, F-69000, Lyon, France

[b] Epigenetics Group, International Agency for Research on Cancer (IARC), Lyon, France.

[c] Département de Chirurgie et Institut de Chirurgie Expérimentale, Centre Léon Bérard, Lyon, France

[d] Hospices Civils de Lyon, Service d'Anatomopathologie, Groupement Hospitalier Lyon Nord, France

[e] Infections and Cancer Biology Group, International Agency for Research on Cancer (IARC), Lyon, France

[f] Hospices Civils de Lyon, Service d'Hépatologie et Gastroentérologie, Groupement Hospitalier Lyon Nord, France

[†] Co-last authors.

* Corresponding author: Dr Claude Caron de Fromentel, UMR INSERM U1052 CNRS5286, Centre de Recherche en Cancérologie de Lyon, 151 cours Albert Thomas, 69424 Lyon Cedex 03, France.

Phone: (+33)472681957; Fax: (+33)472681971; E-mail: claude.de-fromentel@inserm.fr

LIST OF ABBREVIATIONS

AAT, alpha-1 antitrypsin; BSA, bovine serum albumin; CSC, cancer stem cell; CYP3A4, CYP2B6, cytochrome P450 3A4, 2B6; DAPI, 4',6-diamidino-2-phenylindole; DEGs, differentially expressed genes; DLK1, delta-like homolog 1; DMSO, dimethyl sulfoxide; EMT,

epithelial-mesenchymal transition; EpCAM, epithelial cell adhesion molecule; EV, empty vector; FACS, fluorescence-activated cell sorting; FCS, fetal calf serum; HCC, hepatocellular carcinoma; HCV, hepatitis C virus; HNF4, hepatocyte nuclear factor-4; HPV, human papillomavirus; $HRAS^{V12}$, oncogenic Harvey-RAS; hTERT, human telomerase reverse transcriptase subunit; lncRNA, long non-coding RNA; MMLV-RT, Moloney murine leukemia virus-reverse transcriptase; MTS, [3-(4,5-dimethylthiazol-2-yl)-5-(3-carboxymethoxyphenyl)-2-(4-sulfophenyl)-2H-tetrazolium, inner salt]; PBS, phosphate buffered saline; PHH, primary human hepatocytes; PI, propidium iodide; pRb, retinoblastoma protein; RT-qPCR, reverse transcription-quantitative real-time PCR; $SV40^{LT}$, SV40 large T antigen; $SV40^{ST}$, SV40 small T antigen; TAT, tyrosine aminotransferase, TDO, tryptophan 2,3-dioxygenase.

ABSTRACT

Human hepatocarcinogenesis is a complex process with many unresolved issues, including the cell of origin (differentiated and/or progenitor/stem cells) and the initial steps leading to tumor development. With the aim of providing new tools for studying hepatocellular carcinoma initiation and progression, we developed an innovative model based on primary human hepatocytes (PHHs) lentivirus-transduced with $SV40^{LT+ST}$, $HRAS^{V12}$ with or without *hTERT*. The differentiation status of these transduced-PHHs was characterized by RNA sequencing (including lncRNAs), and the expression of some differentiation markers confirmed by RT-qPCR and immunofluorescence. In addition, their transformation capacity was assessed by colony formation in soft agar and tumorigenicity evaluated in immune-deficient mice. The co-expression of $SV40^{LT+ST}$ and $HRAS^{V12}$ in PHHs, in association or not with *hTERT*, led to the emergence of transformed clones. These clones exhibited a poorly differentiated cell phenotype with expression of stemness and mesenchymal-epithelial transition markers and gave rise to cancer stem cell subpopulations. *In vivo*, they resulted in poorly differentiated hepatocellular carcinomas with a reactivation of endogenous *hTERT*. These experiments demonstrate for the first time that non-cycling human mature hepatocytes can be permissive to *in vitro* transformation. This cellular tool provides the first comprehensive *in vitro* model for identifying genetic/epigenetic changes driving human hepatocarcinogenesis.

Key words: hepatocellular carcinoma, transformation, primary human hepatocytes, immature phenotype

INTRODUCTION

Hepatocellular carcinoma (HCC) is a poor prognosis tumor ranking third in terms of the most frequent cause of cancer-related death worldwide[1]. Hepatocarcinogenesis is a complex process combining the accumulation of widely heterogenous genetic and epigenetic changes that occur during the initiation, promotion and progression of the disease. Although common alterations have been identified in tumors[2,3], in human, the early changes leading to the initiation of transformation and the identity of which liver cells (differentiated hepatocytes and/or progenitor/stem cells) are the most permissive to this process are poorly characterized. One reason is the lack of models derived from human hepatocytes. To date, only human pre-immortalized hepatocyte cell lines permissive to the transformation process have been described[4].

One way for driving normal cells to a tumorigenic state *in vitro* is the use of the oncogene combination described by Weinberg and collaborators[5,6]. In this combination, the human telomerase reverse transcriptase subunit (hTERT) immortalizes cells, whereas the SV40 large T antigen ($SV40^{LT}$) binds and inhibits the p53 and pRb tumor suppressors. Finally, the expression of the SV40 small t antigen ($SV40^{ST}$) that indirectly stabilizes C-MYC and of the oncogenic mutant $HRAS^{V12}$ activates mitogenic signaling pathways and promotes cell replication. This results in the emergence of cells with an unlimited replicative potential, partially independent of growth factors, and which have overcome apoptotic and anti-proliferative signals[6]. The oncogene combination described by Weinberg has been used in some human primary cell types including fibroblasts, mammary and bronchial cells, to better characterize the initiation of *in vitro* transformation steps[7]. Numerous cell types of rodent origin, including primary hepatocytes, have also been successfully transformed *in vitro* by the $SV40^{LT}$ and $HRAS^{V12}$ combination. In

mouse, such a strategy has resulted in primary hepatocyte transformation regardless of the cell differentiation state, suggesting that any cell type in the mouse hepatic lineage can initiate HCC[8–10]. With the aim of better characterizing human hepatocarcinogenesis, we have developed the first paradigm of *in vitro* transformation of normal primary human hepatocytes (PHHs).

MATERIALS AND METHODS

Cell culture and transduction

PHHs were isolated from freshly resected non-tumor surrounding liver tissue from three patients undergoing surgery for colorectal adenocarcinoma liver metastasis (Centre Léon Bérard Resource Biological Centre, ministerial agreements #AC-2013-1871 and DC-2013-1870). Signed informed written consent was obtained from patients before surgery. Histological analysis was performed to ensure the absence of microscopic tumor invasion. The two-step collagenase (0.05%, Sigma-Aldrich C5138) perfusion method was used and cells were seeded at confluence in collagen-coated plates[11]. They were maintained for 3 days in William's E medium with GlutaMAX™ (Invitrogen) devoid of fetal calf serum (FCS), supplemented with 100 UI/mL penicillin-G, 100 µg/mL streptomycin, 5 µg/mL insulin, and 5.10^{-5} M hydrocortisone hemisuccinate, and then grown in complete William's E medium containing 10% FCS and 1.8% dimethyl sulfoxide (DMSO). The HuH7 cell line, used as a control in tumorigenicity experiments, was cultured in RPMI-1640 medium supplemented with 10% FCS, 100UI/mL penicillin G, 100 µg/mL streptomycin, 1% non-essential amino acids and 0.01 M Hepes buffer (Invitrogen).

The pLenti6-RAS^{V12} and pLenti6-*hTERT* expression vectors were obtained by inserting the RAS^{V12} cDNA from pBabe-puro RAS^{V12} (Addgene) and the *hTERT* cDNA from pBabe-hygro

hTERT (Addgene) into the pLenti6 lentiviral vector (Invitrogen). pLenti CMV/TO SV40 small t + large T (Addgene) was also used. Virions from lentiviral constructs encoding human *HRAS*^{V12}, SV40^{ST+LT} or *hTERT* were produced in 293FT cells (Invitrogen). PHHs were sequentially transduced (every 7 days) by pLenti CMV/TO SV40^{LT+ST}, pLenti6-*RAS*^{V12} and pLenti6-*hTERT*, at a multiplicity of infection of one (MOI-1) in a medium containing 6 µg/mL polybrene. Cells were then selected with 300 µg/mL geneticin (SV40^{ST+LT}) and/or 3 µg/mL blasticidin (HRAS^{V12}) and/or 200 µg/mL zeocin (hTERT). Lentiviral particles containing empty vector (EV) were used as controls. The efficacy of immortalization was not determined.

RNA extraction, sequencing and real-time quantitative PCR (RT-qPCR)

Total RNA was extracted using Extract-all (Eurobio) from two independent experiments, according to the manufacturer's instructions. Around 3.5 µg of total RNA was ribodepleted using the Ribozero kit (Epicentre) and cDNA libraries for PHH-EV, PHH-SV40^{LT+ST} and PHH-SV40^{LT+ST}/HRAS^{V12} samples were then prepared following the Illumina protocol. Libraries were single-end 50 bp sequenced on an Illumina HiSeq 2500 sequencer. Fastq files underwent a first quality control to assess the quality of sequencing data. Raw reads were aligned on the human genome GRCh38. After filtering non aligned reads or reads with multiple alignments, sequencing depth ranged from 26 to 40 million reads. For RT-qPCR, 1 µg of total RNA was DNase I-digested (Roche), reverse transcribed with random primers and MMLV-RT (Life technologies), and amplified with LightCycler 480 (Roche) using QuantiFast SYBR Green PCR Kit (Qiagen). Levels of gene expression were determined using the Ct method with 18S rRNA as housekeeping gene. Each experiment was conducted three times in triplicate. Oligonucleotide sequences are available on request.

Protein extraction and Western blotting

Proteins were extracted with RIPA [50 mM Tris-HCl, pH 8.0, 150 mM NaCl, 1% Nonidet P-40, 0.5% sodium deoxycholate, 0.1% SDS, 1 mM Na3VO4, protease cocktail inhibitor (Roche)] and protein concentrations were determined using the BCA assay (Pierce). Whole-cell extracts were resolved by SDS-PAGE, transferred onto a PVDF membrane and probed with a specific primary antibody against $SV40^{ST+LT}$ (PAb419, 20% of home-made hybridoma supernatant); HRAS (sc-520, Santa Cruz Biotechnology, 1/1,000); KU80 (AHP317, Serotec, 1/40,000); hTERT (sc-7212, Santa Cruz Biotechnology, 1/500), in 1% w/v nonfat dry milk, 1X TBS, 0.1% Tween-20 at 4°C overnight with gentle shaking. After washing, membranes were incubated with a HRP-conjugated secondary goat anti-rabbit or goat anti-mouse antibody (Sigma, 1/5,000). Protein detection was performed by using the enhanced chemiluminescence kit (Amersham). All blots were standardized for equal protein loading with KU80 staining.

Immunofluorescence

Cells were plated on collagen-coated glass coverslips in a 12-well plate. Twenty four hours later, cells were fixed in 4% paraformaldehyde and permeabilized in PBS containing 0.1% saponin (PBS - 0.1% saponin), for 30 min at room temperature. After saturation in PBS - 0.1% saponin containing 3% BSA, cells were incubated (1 hour at room temperature) with a primary antibody against either VIMENTIN (AC-0024A, 1/400), CK19 (AC-0073A, 1/250), CK18 (AC-001A, 1/500) (Epitomics), CK7 (GA619, Dako, 1/250), ALBUMIN (ab10241, 1/2,000), EpCAM (ab187270, 1/100), CD133 (ab19898, 1/200) (AbCam), or N-Cadherin (14215S; Cell Signaling, 1/200). After washing with PBS - 0.1% saponin, a goat anti-mouse IgG Alexa Fluor 488-conjugated secondary antibody (A-11001) or a goat anti-rabbit IgG Alexa Fluor 555-conjugated secondary antibody (A-21428) (Invitrogen, 1/1,000) was added (30 min / room temperature). Finally, coverslips were washed with PBS - 0.1% saponin, incubated (5 min / room temperature)

with 0.25 µg/mL DAPI prior to mounting in Vectashield medium (Vector Laboratories) and analyzed using a Nikon fluorescence microscope.

Cell growth determination

Growth curves of PHH-SV40^{ST+LT}, PHH-SV40^{ST+LT}/HRAS^{V12} and PHH-SV40^{ST+LT}/HRAS^{V12}/hTERT were compared using MTS assay (CellTiter 96® AQueous One Solution Cell Proliferation Assay, Promega). Cells were seeded at a density of 1.5 x 10^4/cm² in complete medium with 10% FCS. For the 1% FCS cell growth assay, after overnight plating, cells were washed twice in PBS-1X, and complete medium with 1% FCS added to the flasks. The MTS assay was performed daily according to the manufacturer's instructions. Two independent experiments were conducted in triplicate.

Soft agar assay and soft agar colonies isolation

Approximately 5 x 10^3 cells were seeded in 6-cm dishes with culture medium containing 0.35% noble agar, overlaid on culture medium containing 0.7% noble agar and the appropriate selection antibiotics. Liquid medium was refreshed every 5 days and cultures were maintained for 4 weeks when colonies (> 0.15 mm) were then counted. For soft agar colony isolation, macroscopic colonies formed in the semi-solid medium were isolated, trypsinized and re-plated for sub-culture.

Hepatosphere formation

Cells were collected after trypsinization in 15 mL tubes containing 8 mL of complete medium and centrifuged for 5 min at 200 g. The supernatant was discarded and the pellets were resuspended in PBS 1X buffer at 1 x 10^6 cells/mL. For each cell line, cells were then diluted to 1.6 x 10^4 cells/mL in 2 mL of serum-free hepatosphere medium (William's E medium

supplemented with 100 UI/mL penicillin G, 100 µg/mL streptomycin, 1% non-essential amino acids, 0.01 M Hepes buffer, B27 1/50, 10 µg/mL EGF, 20 µg/mL bFGF, 4 µg/mL heparin). 0.5 mL of this dilution was dispensed in two wells of a 24-well ultra-low adherence plate (Costar, Corning), without selection antibiotics. Images of spheres were taken 4 days after seeding. Each condition was performed in duplicate.

Flow cytometry

For cell cycle analysis, cells were harvested in a citrate/sucrose/DMSO buffer 48 h after seeding. Then, RNA was digested and DNA was stained with propidium iodide (PI) (CycleTest Plus kit, Becton Dickinson). The proportion of cells at each cell cycle stage was determined using a FACScan flow cytometer (Becton Dickinson), according to the manufacturer's instructions.

For staining of stem cell-associated markers, cells were harvested by trypsinization in 15 mL tubes containing 8 mL of complete medium and centrifuged for 5 min at 200 g. The supernatant was discarded and the pellets were resuspended in PBS buffer at 1 x 10^6 cells/mL. For each staining condition, 0.5 mL of the cell suspension was dispensed in Eppendorf tubes and centrifuged for 5 min at 400 g. The supernatants were discarded, the pellets resuspended in 100 µL of staining buffer (1X PBS, 2% BSA) and incubated on ice for 10 min for non-specific antigen saturation. For CD44v6, and CD90 detection, the following antibodies were used: CD44v6-FITC (BMS 125FI, eBiosciences), CD90-PE (555596, BD Biosciences), according to manufacturer's instructions. At the end of the incubation period, cells were washed with 1 mL of staining buffer and centrifuged for 5 min at 400 g. Supernatants were discarded and pellets were suspended in 0.5 mL of staining buffer. Cells were incubated with isotype controls (Miltenyi) using the same protocol. Staining analysis was performed with the FACScan flow cytometer (Becton Dickinson), according to the manufacturer's instructions.

Tumorigenicity in nude mice

BALB/c nude mice (Charles River) were maintained in accordance with the Rhone-Alpes ethics committee for animal experimentation and institutional and national guidelines. Transduced-PHHs (1 x 10^6) were implanted subcutaneously into the flanks of 5-week-old female mice. Two independent experiments with two animals were performed per cell line, each animal being injected in each flank, thus being 8 injections per cell line in total. Food and water were given ad libitum. Mice were sacrificed when the tumor size reached 1 cm^3 following ethic committee recommendations, or systematically after 6 months post-injection. Immediately after sacrifice, the tumors were removed and divided into two parts: one piece was frozen in liquid nitrogen, and the second fixed in 4% buffered formalin and paraffin embedded. Sections were cut from the paraffin block and stained with hematoxylin and eosin.

Statistical Analysis

Continuous variables and proportions were compared using the Mann-Whitney (Wilcoxon for paired samples), *t*-Student (paired samples t-test when appropriate) and Chi-squared test. $P < 0.05$ were considered as significant (MedCalc Version 12.7.1.0).

Differential expression analysis and pathway analysis on RNA-sequencing data were performed as previously described[12]. Genes were considered as differentially expressed at family-wise error rate (FWER) < 0.01 (Bonferroni correction) and with absolute fold change higher than 2. Differential gene expression analysis was performed using the R package "edgeR" (R software version 3.1.3)[12]. EdgeR implements an empirical Bayesian method that permits the estimation of gene-specific biological variation, even in the context of minimal levels of biological variation. Heatmaps were used to show differentially expressed genes, using the "heatplot" function of the R package "made4". The function generates an unsupervised hierarchical clustering based on the

gene expression profile of the differentially expressed genes. In order to show an overview of similarities and differences between samples, multi-dimensional scaling plots were obtained using the function "mdsRplot" from the "minfi" R package, using the expression values of the 10% of the most variable genes. Hierarchical clustering based on Euclidian distance was obtained using the function "plotSampleRelation" from the "lumi" R package.

RESULTS

Morphological changes and proliferative capacities of lentiviral-transduced-PHHs

As previously described, PHHs have a considerable replication capacity *in vivo*, but loose this capacity *in vitro*[13]. Freshly isolated PHHs were platted at confluence and monitored using light microscopy. Morphological analysis carried out 7 days after isolation showed cubic binucleated cells that formed a confluent monolayer. By immunofluorescence (IF), PHHs exhibited expression of hepatocyte markers [CK18$^{(+)}$, albumin$^{(+)}$] and absence of cholangiocyte [CK7$^{(-)}$, CK19$^{(-)}$], liver progenitor [EpCAM$^{(-)}$, CD133$^{(-)}$, CK7$^{(-)}$, CK19$^{(-)}$] and mesenchymal cell [vimentin$^{(-)}$] markers (Supplementary Figure 1). After lentiviral transduction of PHHs, the ectopic expression of transgenes was verified by Western-blot analysis (Figure 1A) and their morphology assessed by phase contrast microscopy after three weeks of culture and selection (Figure 1B). PHHs transduced with empty vectors as a negative control (PHH-EV) resembled the parental PHHs, while those transduced with the onco-viral genes SV40^{LT+ST} in association or not with *HRAS^{V12}* and *hTERT* (PHH-SV40^{LT+ST}, PHH-SV40^{LT+ST}/HRAS^{V12}, PHH-SV40^{LT+ST}/HRAS^{V12}/hTERT) displayed a dramatically altered morphology (Figure 1B). PHHs transduced with *HRAS^{V12}* only displayed a morphology resembling oncogene-induced senescence, as previously described[14,15] and no long-term viable cells were obtained (data not

shown). All of the transduced cells expressing SV40^{LT+ST} re-entered the cell cycle, as confirmed by FACS analysis for PHH-SV40^{LT+ST}, PHH-SV40^{LT+ST}/HRAS^{V12} (Figure 2A). The growth rate was similar in PHH-SV40^{LT+ST}, PHH-SV40^{LT+ST}/HRAS^{V12} and PHH-SV40^{LT+ST}/HRAS^{V12}/hTERT when cultured in 10% FCS (Figure 2B). Under conditions of serum starvation (1% FCS), PHH-SV40^{LT+ST} had a reduced growth rate while the PHH-SV40^{LT+ST}/HRAS^{V12} and PHH-SV40^{LT+ST}/HRAS^{V12}/hTERT continued to grow rapidly, indicating a reduced dependence on external mitogen stimuli, one of the hallmarks of *in vitro* transformation (Figure 2C).

In vitro transformation and *in vivo* tumorigenicity of lentiviral transduced-PHHs

The assessment of anchorage-independent growth, another hallmark of *in vitro* transformation, showed that only the combination of SV40^{LT+ST}/*HRAS^{V12}* or SV40^{LT+ST}/*HRAS^{V12}*/*hTERT* expressed in the PHHs was associated with the ability to form colonies greater than 0.15 mm diameter in soft agar (Figure 3A, 3B). The addition of *hTERT*, whilst not required for colony formation, increased the number of colonies (Figure 3B). Six colonies from the PHH-SV40^{LT+ST}/HRAS^{V12} and PHH-SV40^{LT+ST}/HRAS^{V12}/hTERT were isolated and subsequently expanded *in vitro* in 2D-cell subcultures. All the 6 PHH-SV40^{LT+ST}/HRAS^{V12}/hTERT agar colonies grew, but only 2 of the 6 PHH-SV40^{LT+ST}/HRAS^{V12} survived. Indeed, the four others stopped growing and displayed a senescence-like morphology (data not shown). All of the sub-clones that continued to grow were characterized by the same morphology and were able to form anchorage-independent colonies similarly to their parental cells (data not shown).

As the expression of *hTERT* appeared to improve the long-term survival of transduced cells, we evaluated the expression of endogenous *hTERT* in cells not transduced with the *hTERT*-expressing lentivirus. Interestingly, levels of endogenous *hTERT* mRNA increased as the cells

progressed towards a transformed phenotype from PHH-EV to PHH-SV40/ $HRAS^{V12}$, with a maximum in the PHH-SV40/ $HRAS^{V12}$ agar clone, suggesting that the acquisition of *hTERT* expression is critical throughout the transformation process (Figure 4).

Next, the *in vivo* tumorigenic potential of the different transduced cells was tested. 1 x 10^6 PHH-EV, PHH-$SV40^{LT+ST}$ PHH-$SV40^{LT+ST}$/$HRAS^{V12}$ or PHH-$SV40^{LT+ST}$/$HRAS^{V12}$/hTERT cells were subcutaneously injected into immune-deficient nude mice. After three months of monitoring, tumors were detected in all animals injected with PHH-$SV40^{LT+ST}$/$HRAS^{V12}$ or PHH-$SV40^{LT+ST}$/$HRAS^{V12}$/hTERT. In contrast, injection of either 1 x 10^6 PHH-EV or PHH-$SV40^{LT+ST}$ cells failed to give rise to tumors in nude mice during 6 months of follow-up, an observation consistent with previous data obtained from two human immortalized hepatocytic cell lines[4]. Pathological analysis of the tumors revealed a poorly differentiated pattern of HCC infiltrating adjacent tissues (Figure 5A). Tumors with similar features were also observed in mice injected with PHH-$SV40^{LT+ST}$/$HRAS^{V12}$ isolated after two rounds of soft agar growth and sub-culturing. Strikingly, cells derived from these tumors expressed lower mRNA levels of endogenous hTERT than the parental cells (Figure 5B), likely reflecting intra-tumoral heterogeneity. A second tumorigenic assay was performed by using an independent batch of transduced-cell lines, leading to similar results (data not shown).

Transcriptomic analysis

A transcriptomic analysis was carried out to identify the genes with altered expression profiles during the immortalization and transformation processes on two batches of cells from two independent transformation experiments. Since full transformation of PHH- $SV40^{LT+ST}$/$HRAS^{V12}$ was accompanied by an increased expression of endogenous *hTERT*, we did not include the

PHH- SV40^{LT+ST}/HRAS^{V12}/hTERT cells in the analysis. A comparison between the immortalized PHHs (PHH-SV40^{LT+ST}) and PHH-EV cells showed that this process was associated with a dramatic change in gene expression, with 4,003 differentially expressed genes (DEGs) (FWER<0.01, FC>2): 2,139 down-regulated genes in PHH-SV40^{LT+ST} (among which were 186 lncRNAs) and 1,864 up-regulated (135 lncRNAs) compared to PHH-EV (Figure 6A). 1,428 genes were differentially expressed (FWER<0.01, FC>2) in the next transformation stage: 692 genes were down-regulated (40 lncRNAs) and 736 up-regulated (83 lncRNAs) when the profiles of PHH SV40^{LT+ST}/HRAS^{V12} cells were compared to PHH-SV40^{LT+ST} (Figure 6B). Most up-regulated genes showed an increased expression only in the later stages of this immortalization/transformation process with changes being noted only in the PHH-SV40^{LT+ST}/HRAS^{V12} and with no differential expression between the PHH-EV and PHH-SV40^{LT+ST} (Figure 6B). The DEGs clearly clustered in three sub-groups: i) one showing high expression in PHH-EV that was reduced in the PHH-SV40^{LT+ST} and remained low in the PHH-SV40^{LT+ST}/HRAS^{V12}; ii) a second showing an up-regulation only in the PHH-SV40^{LT+ST}; and iii) a third showing a gradual increase in expression as the cells moved from the "normal" phenotype seen in the PHH-EV to intermediate levels in PHH-SV40^{LT+ST} and the highest levels in the fully transformed PHH-SV40^{LT+ST}/HRAS^{V12}.

Pathway analysis showed that genes up-regulated in PHH-SV40^{LT+ST} *vs.* PHH-EV are involved in cell cycle and cell proliferation pathways (including histone coding genes) (Figure 6C). Interestingly, down-regulated genes in PHH-SV40^{LT+ST} were mostly associated with hepatic metabolism. Loss of *HNF4A* expression and its target genes (*ALB*, *CYP450* and coagulation factor genes) indicated that immortalization was associated with a loss of liver cell differentiation (Figure 6D). A comparison between PHH-SV40^{LT+ST}/HRAS^{V12} and PHH-SV40^{LT+ST} transcriptomes revealed that the up-regulated genes were mostly involved in the PI3k-Akt

pathway (Figure 6E) while many down-regulated genes belonged to cell-cell interaction pathways, although this trend was not consistent across the different queried databases (Figure 6F). Taken together, these results suggest that these two pathways are critical to induce the transformation of immortalized cells.

Most of the altered long non-coding RNAs (lncRNAs) were up-regulated during the transition from immortalized PHH-SV40^{LT+ST} towards the transformed PHH-SV40^{LT+ST}/HRAS^{V12} (Supplementary Figure 2). The majority of them have not previously been identified associated with HCC, although several have been described to be cancer-related (for example CCAT, CRNDE, LUCAT1, CASC8, CASC19). In contrast, HOTAIR, a well-known cancer promoting lncRNA, was up-regulated in the immortalized PHH-SV40^{LT+ST} suggesting that its up-regulation is an early event in HCC development. These data showed that the PHH-EV cells clustered and were distinct from the immortalized (PHH-SV40^{LT+ST}) and transformed cells (PHH-SV40^{LT+ST}/HRAS^{V12}) (Figure 7A, 7B).

Immortalization and transformation of PHH is associated with a dedifferentiation process

As suggested by the large-scale transcriptome analysis, hepatocyte dedifferentiation occurred during the immortalization/transformation process as confirmed by the dramatic changes in the expression of a panel of genes by RT-qPCR (Table 1). In comparison with PHH-EV cells, the PHH-SV40^{LT+ST} and PHH-SV40^{LT+ST}/HRAS^{V12} harbored a striking decrease in hepatocyte-specific markers: *ALBUMIN*, *AAT*, *CYP3A4*, *CYP2B6*, *HNF4*, *TAT*, *TDO*. The levels of the epithelial marker *KRT18* were already lowered in the PHH-SV40^{LT+ST} and showed no further decrease in the PHH-SV40^{LT+ST}/HRAS^{V12} while the levels of the progenitor cell marker *KRT19* were high in the immortalized PHH-SV40^{LT+ST} and low in the poorly differentiated transformed

PHH-SV40^{LT+ST}/HRAS^{V12} cells. Changes in the balance of several epithelial and hepatocyte markers were confirmed at the protein level by immunofluorescence in the PHH-SV40^{LT+ST} and PHH-SV40^{LT+ST}/HRAS^{V12} cells (Figure 8) in comparison with PHHs (Supplementary Figure 1). Indeed, a sequential decrease of Albumin and CK18 (hepatocyte and epithelial markers) and the appearance of vimentin and N-cadherin (mesenchymal markers) were noted. In addition, CK19 progenitor marker was up-regulated in PHH-SV40^{LT+ST} and its expression lost in PHH-SV40^{LT+ST}/HRAS^{V12} cells. Similar data were observed at the mRNA level in HCC tumors growing after heterotopic injection in nude mice (Table 2).

Transformation of PHHs is associated with the acquisition of stemness markers and cancer stem cell (CSC) properties

As assessed by RT-qPCR, stemness markers such as *DLK1*, *EpCAM*, *BMI*, *NANOG*, *OCT4*, and *SOX2* were mainly up-regulated in transformed PHH-SV40^{LT+ST}/HRas^{V12} compared to PHH-EV and were absent or modestly over-expressed in immortalized PHH-SV40^{LT+ST}. However, *FZD7* and *ΔNp73*, associated to immaturity in several tissues[16–19], were strikingly up-regulated in the early steps of transformation, as suggested by an up-regulation in PHH-SV40^{LT+ST} and remained at higher levels in our model of fully transformed cells (PHH-SV40^{LT+ST}/HRAS^{V12}) (Table 1). FACS analysis showed that PHH-SV40^{LT+ST} and PHH-SV40^{LT+ST}/HRAS^{V12} carried the CD90 surface stemness marker as well as ALDH labeling, whereas they were both negative for the stemness-associated marker CD44v6 (Supplementary Figure 3). Confirming the increased stem-like phenotype of PHH-SV40^{LT+ST}/HRAS^{V12}, only these cells could give rise to hepatospheres in low attachment conditions, a classical assay for assessing stem cells (Figure 9A, 9B). Overall, these *in vitro* molecular and cellular characterizations indicate that dedifferentiation accompanied the immortalization step and was reinforced during full transformation.

DISCUSSION

This study reports the use of normal differentiated adult hepatocytes of human origin (PHHs) to establish a model of *in vitro* human hepatocarcinogenesis in which we strikingly found that resulting HCC cells exhibited some features of immaturity and CSC-like properties.

While it is clear that cancers arise from the accumulation of genetic and/or epigenetic abnormalities that endow the malignant cell with the properties of uncontrolled growth and proliferation, the precise sequence of these events that program human hepatocarcinogenesis remains heterogeneous and unclear. That is why the generation of new models of transformation is needed. The use of oncogenic proteins derived from DNA tumor viruses in experimental models of transformation has provided fundamental insight into the process of cell transformation over the last decades. In 1999, Weinberg and collaborators reported for the first time that the co-expression of $SV40^{LT}$ and $SV40^{ST}$, *hTERT*, and $HRAS^{V12}$ in normal human fibroblasts and kidney cells converted them into tumorigenic cells[5]. However, this has never been investigated in hepatocytes. The *in vitro* transformation of hepatocytes of human origin has previously been reported although the cells used were not normal quiescent hepatocytes, but the pre-immortalized HL-7702 and HL-7703 cell lines, transformed either by the $SV40^{LT+ST}$/*RAS*/*hTERT* combination[4] or *RhoC*[20]. In the present study, we show for the first time that $SV40^{LT+ST}$ co-expression immortalizes primary human liver cells and that the addition of $HRAS^{V12}$ transforms these cells. This process required the reactivation of telomerase either by spontaneous upregulation of the endogenous *hTERT* or directly by lentiviral transduction of *hTERT*. Transcriptome analysis showed that immortalization induced the greatest change in the gene expression profiles with a partial loss of cell identity, including a decrease in hepatocyte markers,

such as *ALBUMIN*, *CYP* genes, coagulation factors and lineage-specific transcription factors (e.g. *HNF4A*).

Although being a key driver of cancer development[21], the ectopic expression of *HRAS* alone mainly provokes oncogene-induced senescence by activating the p53/pRb gatekeepers, which serve as a major barrier to Ras-driven transformation in different types of cells including hepatocytes[14,15]. Indeed, in our model, the ectopic expression of $HRAS^{V12}$ alone, without previous immortalization by $SV40^{LT+ST}$, resulted in non-proliferative cells with a morphology reminiscent of senescence, strengthening the need of immortalization prior to transformation as has been reported in many models[22,23]. In contrast, $SV40^{LT+ST}$ expression allowed the quiescent PHHs to re-enter the cell cycle and reach immortalization, as described with other proteins such as HCV core or HPV E6-E7[24,25]. It is well established that expression of $SV40^{LT}$ in combination with an oncogenic allele of HRAS is sufficient to transform normal rodent cells[26] including hepatocytes[10]. One of the mechanisms involved is the inactivation of the p53 and retinoblastoma (pRb) tumor suppressor proteins through their interaction with $SV40^{LT}$. However, similar attempts to transform normal cells of human origin through immortalization with $SV40^{LT}$ alone, have mostly failed due to the cells entering an irreversible growth arrest or undergoing apoptosis[27]. Interestingly, $SV40^{ST}$ is able to boost $SV40^{LT}$ expression[28]. This could, for instance, perturb the expression of the phosphatase 2A protein[6], and allow the $SV40^{LT}$-mediated inhibition of p53 that has been shown to contribute to the acquisition and/or maintenance of CSC properties[29] in addition to cell transformation.

We found that, among the lentiviral-transduced PHHs giving rise to colonies in soft agar, all the PHH-$SV40^{LT+ST}$/$HRAS^{V12}$/hTERT-derived colonies were able to grow after subsequent subculture, whereas only one third of the PHH-$SV40^{LT+ST}$/$HRAS^{V12}$-derived colonies displayed this ability. These latter colonies showed reactivation of the endogenous *hTERT*, thus preventing

replicative senescence and enhancing the transformation process. The role of telomerase expression as an essential requirement for the neoplastic conversion of human cells is controversial. In models in which normal human cells were converted to cancer cells by the combination of SV40 and oncogenic *RAS*, *hTERT* was originally described as essential[5]. In other approaches using primary cultures of colon smooth muscle cells isolated from surgical specimens, ectopic SV40 and oncogenic *HRAS* rapidly transformed the cells growing *in vitro*, which were tumorigenic in immune-deficient mice without a previous selection in culture[30]. However, the cells in the resulting cancers showed morphological evidence of crisis, consistent with their lack of telomerase, thus supporting the concept that $HRAS^{V12}$ and SV40 form a minimal set of genes that can convert normal human cells into cancer cells without a requirement for *hTERT*[30]. Another hypothesis would be that the $SV40^{LT+ST}$ and $HRAS^{V12}$ combination is able to reactivate the endogenous telomerase, either by direct impact or in a stepwise manner as described in mammary models of transformation driven by Wnt signaling[31]. Our data could support this last hypothesis in a hepatic model.

It is recognized that both the cell of origin and the type of cancer-predisposing genomic/epigenomic alterations contribute to the phenotypic and molecular diversity of HCC. The numerous experimental rodent models developed these last ten years support either progenitors or mature hepatocytes as the cell of origin of HCC, depending on the modified signaling pathway[32–36]. Unfortunately, most of these models are far from human hepatocarcinogenesis and additional studies and models are needed to fill the gap between findings obtained in animals and studies of patients with liver tumors[37,38].

By using the $SV40^{LT}$/$HRas^{V12}$ combination to induce *in vitro* transformation of mouse liver cells, Holczbauer and collaborators provided conclusive evidence that the acquisition of stemness properties in HCCs is independent of the cell of origin [10]. In their model, the expression of both

SV40^{LT} and oncogenic *HRas^{V12}* forced diverse hepatic cell lineages (primary hepatic progenitor cells, lineage-committed hepatoblasts and differentiated mature adult hepatocytes) to reprogram into HCC cells with some stemness and EMT traits, as also found in human tumors[39,40]. They also reported that HCC cells generation from adult mouse hepatocytes required the expression of *c-Myc*[10]. In our human HCC model, we were unable to identify the cell of origin, despite the identification of some stemness and EMT traits, together with the unchanged expression of *C-MYC* (data not shown). Additional experiments using reporter genes under the control of promoters activated in hepatic progenitors or mature hepatocytes could provide new information on the cell of origin. However, such markers specific to hepatic progenitors remain to be identified so far.

In conclusion, we have generated for the first time an *in vitro* model of immortalization and transformation from human adult mature hepatocytes that provides a useful tool for studying the molecular and cellular events involved in hepatocarcinogenesis. This proof of concept model with the well-established SV40 and *HRAS* combination could provide the experimental basis for the assessment of the contribution of other genetic and epigenetic changes implicated in human hepatocarcinogenesis and provides an assay system for the development of more effective therapeutic strategies.

AUTHOR CONTRIBUTIONS: F.P., P.G., D.D-E., N.F., A.L., L.L., M.M. performed experiments and data analysis. M.R. provided patients' samples. B.B. performed the histological analysis of mice tumors. B.S. and Z.H. were involved in the design of the study and revised the manuscript. F.P., C.C.F. and P.M. designed the study, analyzed data and wrote the paper.

ACKNOWLEDGEMENTS: RNA-sequencing was performed at the platform "Biopuce et sequençage" of the Institut de Biologie Moléculaire and Cellulaire, Strasbourg. The authors thank Sabrina Chesnais for her support in mice injections and Janet Hall and Brigitte Manship for helpful discussions and English proofreading.

FUNDING: This work was supported by the French Institut National du Cancer (INCA) (grant contract #2009-143, PAIR-CHC 2009) and the French Ligue Nationale Contre le Cancer (LNCC). F Pez and N Fares were supported by the French National Institute du Cancer (INCA), A Lopez by the French Ligue Nationale Contre le Cancer (LNCC), and P Gifu by the IMODI consortium.

CONFLICT OF INTEREST: Authors have no competing financial interest in relation to the work described.

REFERENCES

[1] J. Ferlay, M. Colombet, I. Soerjomataram, C. Mathers, D.M. Parkin, M. Piñeros, A. Znaor, F. Bray, Estimating the global cancer incidence and mortality in 2018: GLOBOCAN sources and methods, Int. J. Cancer. (2018). doi:10.1002/ijc.31937.

[2] P.A. Farazi, R.A. DePinho, Hepatocellular carcinoma pathogenesis: from genes to environment, Nat. Rev. Cancer. 6 (2006) 674–687. doi:10.1038/nrc1934.
[3] J. Zucman-Rossi, A. Villanueva, J.-C. Nault, J.M. Llovet, Genetic Landscape and Biomarkers of Hepatocellular Carcinoma, Gastroenterology. 149 (2015) 1226-1239.e4. doi:10.1053/j.gastro.2015.05.061.
[4] B. Sun, M. Chen, C. Hawks, P.J. Hornsby, X. Wang, Tumorigenic study on hepatocytes coexpressing SV40 with Ras, Mol. Carcinog. 45 (2006) 213–219. doi:10.1002/mc.20137.
[5] W.C. Hahn, C.M. Counter, A.S. Lundberg, R.L. Beijersbergen, M.W. Brooks, R.A. Weinberg, Creation of human tumour cells with defined genetic elements, Nature. 400 (1999) 464–468. doi:10.1038/22780.
[6] W.C. Hahn, S.K. Dessain, M.W. Brooks, J.E. King, B. Elenbaas, D.M. Sabatini, J.A. DeCaprio, R.A. Weinberg, Enumeration of the simian virus 40 early region elements necessary for human cell transformation, Mol. Cell. Biol. 22 (2002) 2111–2123.
[7] W.C. Hahn, Experimental models of human cancer, Cell Cycle Georget. Tex. 3 (2004) 604–605. doi:10.4161/cc.3.5.836.
[8] H.C. Isom, C.D. Woodworth, Y. Meng, J. Kreider, T. Miller, L. Mengel, Introduction of the ras oncogene transforms a simian virus 40-immortalized hepatocyte cell line without loss of expression of albumin and other liver-specific genes, Cancer Res. 52 (1992) 940–948.
[9] J.R. Jacob, B.C. Tennant, Transformation of immortalized woodchuck hepatic cell lines with the c-Ha-ras proto-oncogene, Carcinogenesis. 17 (1996) 631–636.
[10] Á. Holczbauer, V.M. Factor, J.B. Andersen, J.U. Marquardt, D.E. Kleiner, C. Raggi, M. Kitade, D. Seo, H. Akita, M.E. Durkin, S.S. Thorgeirsson, Modeling pathogenesis of primary liver cancer in lineage-specific mouse cell types, Gastroenterology. 145 (2013) 221–231. doi:10.1053/j.gastro.2013.03.013.
[11] P. Gripon, C. Diot, C. Guguen-Guillouzo, Reproducible high level infection of cultured adult human hepatocytes by hepatitis B virus: effect of polyethylene glycol on adsorption and penetration, Virology. 192 (1993) 534–540. doi:10.1006/viro.1993.1069.
[12] D.D. Esposti, H. Hernandez-Vargas, C. Voegele, N. Fernandez-Jimenez, N. Forey, B. Bancel, F. Le Calvez-Kelm, J. McKay, P. Merle, Z. Herceg, Identification of novel long non-coding RNAs deregulated in hepatocellular carcinoma using RNA-sequencing, Oncotarget. 7 (2016) 31862–31877. doi:10.18632/oncotarget.7364.
[13] J. Shan, R.E. Schwartz, N.T. Ross, D.J. Logan, D. Thomas, S.A. Duncan, T.E. North, W. Goessling, A.E. Carpenter, S.N. Bhatia, Identification of small molecules for human hepatocyte expansion and iPS differentiation, Nat. Chem. Biol. 9 (2013) 514–520. doi:10.1038/nchembio.1270.
[14] M. Serrano, A.W. Lin, M.E. McCurrach, D. Beach, S.W. Lowe, Oncogenic ras provokes premature cell senescence associated with accumulation of p53 and p16INK4a, Cell. 88 (1997) 593–602.
[15] H. Donninger, D.F. Calvisi, T. Barnoud, J. Clark, M.L. Schmidt, M.D. Vos, G.J. Clark, NORE1A is a Ras senescence effector that controls the apoptotic/senescent balance of p53 via HIPK2, J. Cell Biol. 208 (2015) 777–789. doi:10.1083/jcb.201408087.
[16] C.O.-N. Leung, W.-N. Mak, A.K.-L. Kai, K.-S. Chan, T.K.-W. Lee, I.O.-L. Ng, R.C.-L. Lo, Sox9 confers stemness properties in hepatocellular carcinoma through Frizzled-7 mediated Wnt/β-catenin signaling, Oncotarget. 7 (2016) 29371–29386. doi:10.18632/oncotarget.8835.
[17] G. Li, Q. Su, H. Liu, D. Wang, W. Zhang, Z. Lu, Y. Chen, X. Huang, W. Li, C. Zhang, Y. He, L. Fu, J. Bi, Frizzled7 Promotes Epithelial-to-mesenchymal Transition and Stemness

Via Activating Canonical Wnt/β-catenin Pathway in Gastric Cancer, Int. J. Biol. Sci. 14 (2018) 280–293. doi:10.7150/ijbs.23756.
[18] C. Meier, P. Hardtstock, S. Joost, V. Alla, B.M. Pützer, p73 and IGF1R Regulate Emergence of Aggressive Cancer Stem-like Features via miR-885-5p Control, Cancer Res. 76 (2016) 197–205. doi:10.1158/0008-5472.CAN-15-1228.
[19] T. Voeltzel, M. Flores-Violante, F. Zylbersztejn, S. Lefort, M. Billandon, S. Jeanpierre, S. Joly, G. Fossard, M. Milenkov, F. Mazurier, A. Nehme, A. Belhabri, E. Paubelle, X. Thomas, M. Michallet, F. Louache, F.-E. Nicolini, C. Caron de Fromentel, V. Maguer-Satta, A new signaling cascade linking BMP4, BMPR1A, ΔNp73 and NANOG impacts on stem-like human cell properties and patient outcome, Cell Death Dis. 9 (2018) 1011. doi:10.1038/s41419-018-1042-7.
[20] S. Xie, M. Zhu, G. Lv, Y. Geng, G. Chen, J. Ma, G. Wang, Overexpression of Ras homologous C (RhoC) induces malignant transformation of hepatocytes in vitro and in nude mouse xenografts, PloS One. 8 (2013) e54493. doi:10.1371/journal.pone.0054493.
[21] G. De Vita, L. Bauer, V.M.C. da Costa, M. De Felice, M.G. Baratta, M. De Menna, R. Di Lauro, Dose-dependent inhibition of thyroid differentiation by RAS oncogenes, Mol. Endocrinol. Baltim. Md. 19 (2005) 76–89. doi:10.1210/me.2004-0172.
[22] R.F. Newbold, R.W. Overell, J.R. Connell, Induction of immortality is an early event in malignant transformation of mammalian cells by carcinogens, Nature. 299 (1982) 633–635.
[23] X. Yuan, C. Larsson, D. Xu, Mechanisms underlying the activation of TERT transcription and telomerase activity in human cancer: old actors and new players, Oncogene. 38 (2019) 6172–6183. doi:10.1038/s41388-019-0872-9.
[24] R.B. Ray, K. Meyer, R. Ray, Hepatitis C virus core protein promotes immortalization of primary human hepatocytes, Virology. 271 (2000) 197–204. doi:10.1006/viro.2000.0295.
[25] Y. Tsuruga, T. Kiyono, M. Matsushita, T. Takahashi, H. Kasai, S. Matsumoto, S. Todo, Establishment of immortalized human hepatocytes by introduction of HPV16 E6/E7 and hTERT as cell sources for liver cell-based therapy, Cell Transplant. 17 (2008) 1083–1094.
[26] D. Michalovitz, L. Fischer-Fantuzzi, C. Vesco, J.M. Pipas, M. Oren, Activated Ha-ras can cooperate with defective simian virus 40 in the transformation of nonestablished rat embryo fibroblasts, J. Virol. 61 (1987) 2648–2654.
[27] R. Sager, K. Tanaka, C.C. Lau, Y. Ebina, A. Anisowicz, Resistance of human cells to tumorigenesis induced by cloned transforming genes, Proc. Natl. Acad. Sci. U. S. A. 80 (1983) 7601–7605.
[28] T. Kolzau, R.S. Hansen, D. Zahra, R.R. Reddel, A.W. Braithwaite, Inhibition of SV40 large T antigen induced apoptosis by small T antigen, Oncogene. 18 (1999) 5598–5603. doi:10.1038/sj.onc.1202942.
[29] L. Yi, C. Lu, W. Hu, Y. Sun, A.J. Levine, Multiple roles of p53-related pathways in somatic cell reprogramming and stem cell differentiation, Cancer Res. 72 (2012) 5635–5645. doi:10.1158/0008-5472.CAN-12-1451.
[30] S. Liang, M.S. Kahlenberg, D.L. Rousseau, P.J. Hornsby, Neoplastic conversion of human colon smooth muscle cells: No requirement for telomerase, Mol. Carcinog. 47 (2008) 478–484. doi:10.1002/mc.20405.
[31] A. Ayyanan, G. Civenni, L. Ciarloni, C. Morel, N. Mueller, K. Lefort, A. Mandinova, W. Raffoul, M. Fiche, G.P. Dotto, C. Brisken, Increased Wnt signaling triggers oncogenic conversion of human breast epithelial cells by a Notch-dependent mechanism, Proc. Natl. Acad. Sci. U. S. A. 103 (2006) 3799–3804. doi:10.1073/pnas.0600065103.

[32] T. Roskams, Liver stem cells and their implication in hepatocellular and cholangiocarcinoma, Oncogene. 25 (2006) 3818–3822. doi:10.1038/sj.onc.1209558.
[33] L. Lu, Y. Li, S.M. Kim, W. Bossuyt, P. Liu, Q. Qiu, Y. Wang, G. Halder, M.J. Finegold, J.-S. Lee, R.L. Johnson, Hippo signaling is a potent in vivo growth and tumor suppressor pathway in the mammalian liver, Proc. Natl. Acad. Sci. U. S. A. 107 (2010) 1437–1442. doi:10.1073/pnas.0911427107.
[34] S. Benhamouche, M. Curto, I. Saotome, A.B. Gladden, C.-H. Liu, M. Giovannini, A.I. McClatchey, Nf2/Merlin controls progenitor homeostasis and tumorigenesis in the liver, Genes Dev. 24 (2010) 1718–1730. doi:10.1101/gad.1938710.
[35] S. Shin, K.J. Wangensteen, M. Teta-Bissett, Y.J. Wang, E. Mosleh-Shirazi, E.L. Buza, L.E. Greenbaum, K.H. Kaestner, Genetic lineage tracing analysis of the cell of origin of hepatotoxin-induced liver tumors in mice, Hepatology. 64 (2016) 1163–1177. doi:10.1002/hep.28602.
[36] X. Mu, R. Español-Suñer, I. Mederacke, S. Affò, R. Manco, C. Sempoux, F.P. Lemaigre, A. Adili, D. Yuan, A. Weber, K. Unger, M. Heikenwälder, I.A. Leclercq, R.F. Schwabe, Hepatocellular carcinoma originates from hepatocytes and not from the progenitor/biliary compartment, J. Clin. Invest. 125 (2015) 3891–3903. doi:10.1172/JCI77995.
[37] D. Sia, A. Villanueva, S.L. Friedman, J.M. Llovet, Liver Cancer Cell of Origin, Molecular Class, and Effects on Patient Prognosis, Gastroenterology. 152 (2017) 745–761. doi:10.1053/j.gastro.2016.11.048.
[38] T.N. Flores-Téllez, S. Villa-Treviño, C. Piña-Vázquez, Road to stemness in hepatocellular carcinoma, World J. Gastroenterol. 23 (2017) 6750–6776. doi:10.3748/wjg.v23.i37.6750.
[39] K. Polyak, R.A. Weinberg, Transitions between epithelial and mesenchymal states: acquisition of malignant and stem cell traits, Nat. Rev. Cancer. 9 (2009) 265–273. doi:10.1038/nrc2620.
[40] J.Y. Seok, D.C. Na, H.G. Woo, M. Roncalli, S.M. Kwon, J.E. Yoo, E.Y. Ahn, G.I. Kim, J.-S. Choi, Y.B. Kim, Y.N. Park, A fibrous stromal component in hepatocellular carcinoma reveals a cholangiocarcinoma-like gene expression trait and epithelial-mesenchymal transition, Hepatol. Baltim. Md. 55 (2012) 1776–1786. doi:10.1002/hep.25570.

FIGURE LEGEND

Figure 1. Characterization of lentiviral-transduced PHH-EV, PHH-SV40^{LT+ST}, PHH-SV40^{LT+ST}/HRAS^{V12} and PHH-SV40^{LT+ST}/HRAS^{V12}/hTERT cells. PHHs were sequentially transduced with SV40 early region (LT+ST), *HRAS^{V12}* and *hTERT*. (A) The transgene intracellular levels were evaluated by Western blot analysis on the total protein lysate. The anti-SV40 antibody binds both large T (LT) and small t (ST) viral antigens. The anti-HRAS antibody binds both the ectopic mutated HRAS^{V12} and the endogenous wild-type HRAS proteins. The anti-hTERT antibody binds the catalytic subunit of human telomerase. Ku80 was used as a loading control. MW, molecular weight; EV, empty vector. (B) Phase-contrast microscopy reveals a hepatocyte morphology for the PHH-EV cells, whereas PHH-SV40^{LT+ST}, PHH-SV40^{LT+ST}/HRAS^{V12} and PHH-SV40^{LT+ST}/HRAS^{V12}/hTERT resemble epithelial non-hepatocyte cells. Pictures are representative of those obtained in three independent experiments (magnification, upper panel 200x, lower panel 400x).

Figure 2. Cell cycle and proliferation analyses of the lentiviral-transduced PHH-SV40^{LT+ST}, PHH-SV40^{LT+ST}/HRAS^{V12}and PHH-SV40^{LT+ST}/HRAS^{V12}/hTERT cells. (A) Propidium iodide staining and FACS analysis show that PHH-SV40^{LT+ST} and PHH-SV40^{LT+S}/HRAS^{V12} cells are actively cycling (n=3). PHH-EV are not shown since non-cycling. (B) Cell growth, as evaluated by MTS assay, of PHH-SV40^{LT+ST}, PHH-SV40^{LT+ST}/HRAS^{V12} and PHH-SV40^{LT+ST}/HRAS^{V12}/hTERT cells is similar in the presence of 10% FCS, but (C) only PHHs expressing *HRAS^{V12}* show a significant growth in serum-deprived medium. Non-parametric Mann-Whitney test between PHH-SV40^{LT+ST}/HRAS^{V12} and PHH-SV40^{LT+ST} was used for each time-point, from two independent experiments conducted in triplicate, (*) $P < 0.05$.

Figure 3. PHH-EV, PHH-SV40^{LT+ST}, PHH-SV40^{LT+ST}/HRAS^{V12} and PHH-SV40^{LT+ST}/HRAS^{V12}/hTERT growth in anchorage-independent conditions. (A) Microscopic view of colonies from soft agar assays in 6-well plates (magnification, 100x). (B) Only colonies with a diameter > 0.15 mm - were counted. Data represent the mean of four independent experiments in duplicate. Non-parametric Mann-Whitney test; * $P < 0.05$.

Figure 4. Expression of endogenous *hTERT* in PHH, PHH-SV40^{LT+ST} and PHH-SV40^{LT+ST}/HRAS^{V12} cells. Endogenous hTERT expression, assessed by RT-qPCR, increases from PHH-EV to PHH-SV40^{LT+ST}/HRAS^{V12} cells, reaching a maximum in PHH-SV40^{LT+ST}/HRAS^{V12} cells isolated from agar clones and plated in 2D culture. Data represent the mean of eight independent experiments in duplicate. Non-parametric Mann-Whitney test; * $P < 0.05$, ** $P<0.01$.

Figure 5. Tumorigenic potential of PHH-SV40^{LT+ST}/HRAS^{V12}. (A) Histological examination of PHH-SV40^{LT+ST}/HRAS^{V12}-derived tumors reveals a poorly differentiated HCC with a solid trabecular pattern, which infiltrates the hypoderm and muscle tissues (hematoxylin and eosin (H&E) staining, magnification 100x) (upper panel). Higher magnification image details morphology showing abundant eosinophilic cytoplasm and irregular pleomorphic nuclei with distinct nucleoli, numerous mitosis (some of them being atypical), absence of glycogen, bile pigment, or steatosis (H&E, magnification 400x) (lower panel). (B) Tumor cells from PHH-SV40^{LT+ST}/HRAS^{V12} agar clone do not express more endogenous hTERT than the parental cells, as evaluated by RT-qPCR. Data represent the mean of four independent experiments in duplicate. Non-parametric Mann-Whitney test; * $P < 0.05$.

Figure 6. Comparison of PHH-EV, PHH-SV40^{LT+ST} and PHH-SV40 $^{LT+ST}$/HRAS^{V12} transcriptomes. (A) Comparison of transcriptome between two batches of cells, using PHH-EV as a reference; 2,139 genes are down-regulated and 1,864 up-regulated in PHH-SV40^{LT+ST} compared to PHH-EV, fold change > 2, Bonferroni adjusted p-value FWER < 0.01. (B) Comparison between two batches of cells using PHH-SV40^{LT+ST} as a reference; 692 genes are down-regulated and 736 up-regulated in PHH-SV40^{LT+ST}/HRAS^{V12}, compared to PHH-SV40^{LT+ST}, fold change > 2, Bonferroni adjusted p-value FWER < 0.01. (C) Up-regulated genes and (D) down-regulated genes in PHH-SV40^{LT+ST} *vs*. PHH-EV. (E) Up-regulated genes and (F) down-regulated genes in PHH-SV40^{LT+ST}/HRAS^{V12} *vs.* PHH-SV40^{LT+ST}. Differential gene expression analysis was performed using the R package "edgeR" (R software version 3.1.3).

Figure 7. Clustering of PHH-EV, PHH-SV40^{LT+ST} and transformed PHH-SV40^{LT+ST}/HRAS^{V12}. (A) Clustering based on whole transcriptome with sample relations based on 17,727 genes. (B) MDS plot based on the 10% most variable genes (MDS 1,773 most variable positions). Both analyses clearly show that PHH-EV (PHH on the figure) clustered separately to the two other cell lines.

Figure 8. Expression of some phenotypic markers in PHH-SV40^{LT+ST} and PHH-SV40^{LT+ST}/HRAS^{V12}. Cells were assessed for different markers by indirect immunofluorescence: Albumin and CK18 for hepatocyte lineage, CK19 for cholangiocyte or hepatic progenitor lineage, N-cadherin and vimentin as mesenchymal markers. Double staining of albumin and vimentin was performed to evaluate the proportion of cell harboring an epithelial or mesenchymal phenotype. Double staining of N-cadherin and vimentin confirmed that almost all

cells have acquired mesenchymal markers. Nuclei were stained by DAPI (blue). Pictures are representative of those obtained in three independent experiments (magnification, 200x).

Figure 9. Capacity of PHH-SV40^{LT+ST}/HRAS^{V12} to form hepatospheres. Cells were cultured in low attachment conditions. Pre-agar or post-agar 2D-cultured PHH-SV40^{LT+ST}/HRAS^{V12} cells were able to form large size (> 80 µm) hepatospheres. In contrast, PHH-SV40^{LT+ST} formed small size hepatospheres only. (A) Pictures were taken after 4 days culture (magnification, 40x). (B) Hepatospheres > 80 µm diameter were counted in each well (2 independent experiments in duplicate) and the mean +/- SEM was calculated.

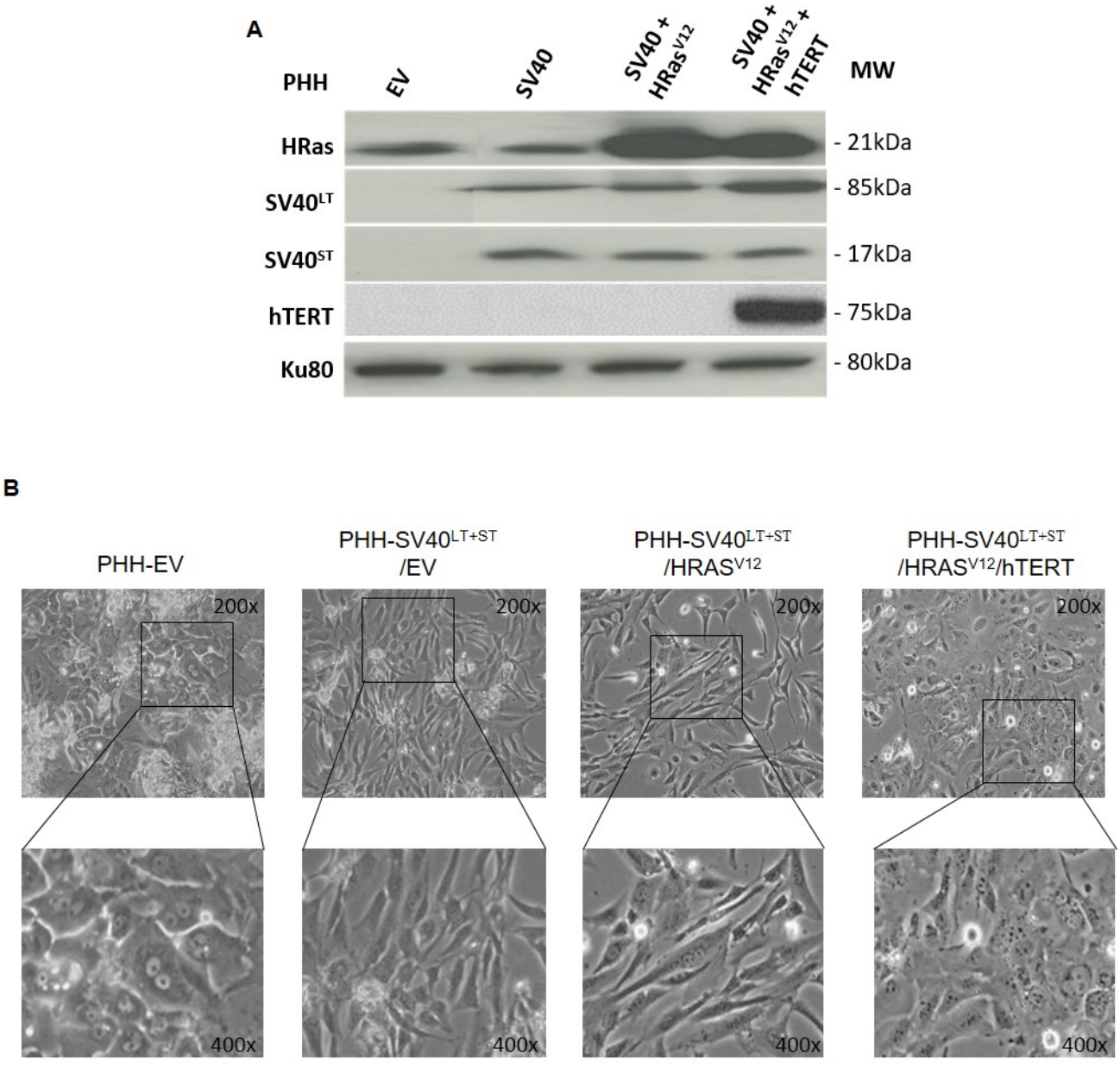
A
PHH
EV
SV40
SV40 + HRasV12
SV40 + HRasV12 + hTERT
MW
HRas
- 21kDa
SV40LT
- 85kDa
SV40ST
- 17kDa
hTERT
- 75kDa
Ku80
- 80kDa
B
PHH-EV
PHH-SV40LT+ST /EV
PHH-SV40LT+ST /HRASV12
PHH-SV40LT+ST /HRASV12/hTERT
200x
400x

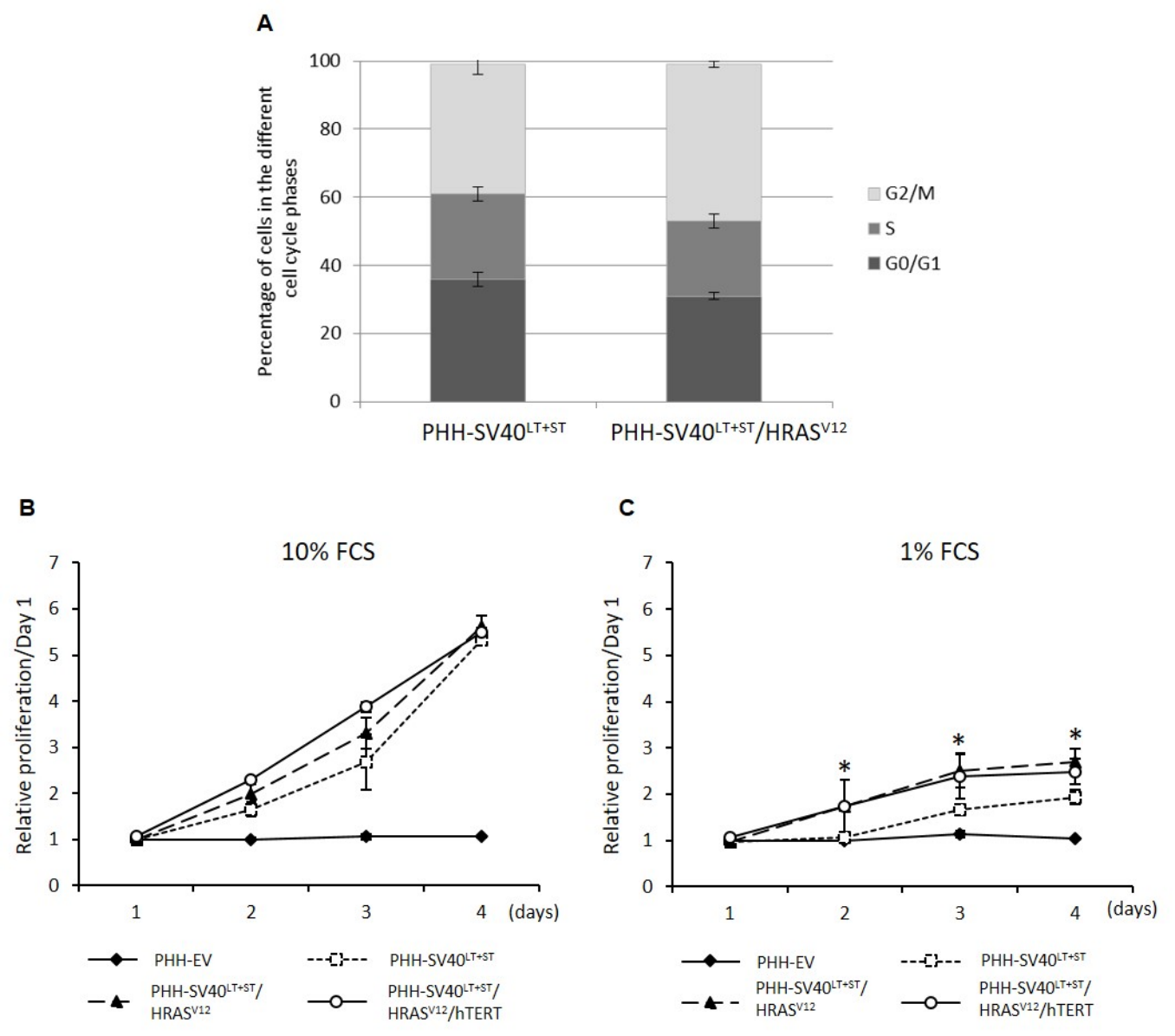
A
Percentage of cells in the different cell cycle phases
100
80
60
40
20
0
G2/M
S
G0/G1
PHH-SV40LT+ST
PHH-SV40LT+ST/HRASV12
B
10% FCS
Relative proliferation/Day 1
7
6
5
4
3
2
1
0
1
2
3
4
(days)
PHH-EV
PHH-SV40LT+ST
PHH-SV40LT+ST/ HRASV12
PHH-SV40LT+ST/ HRASV12/hTERT
C
1% FCS
Relative proliferation/Day 1
7
6
5
4
3
2
1
0
1
2
3
4
(days)
*
*
*
PHH-EV
PHH-SV40LT+ST
PHH-SV40LT+ST/ HRASV12
PHH-SV40LT+ST/ HRASV12/hTERT

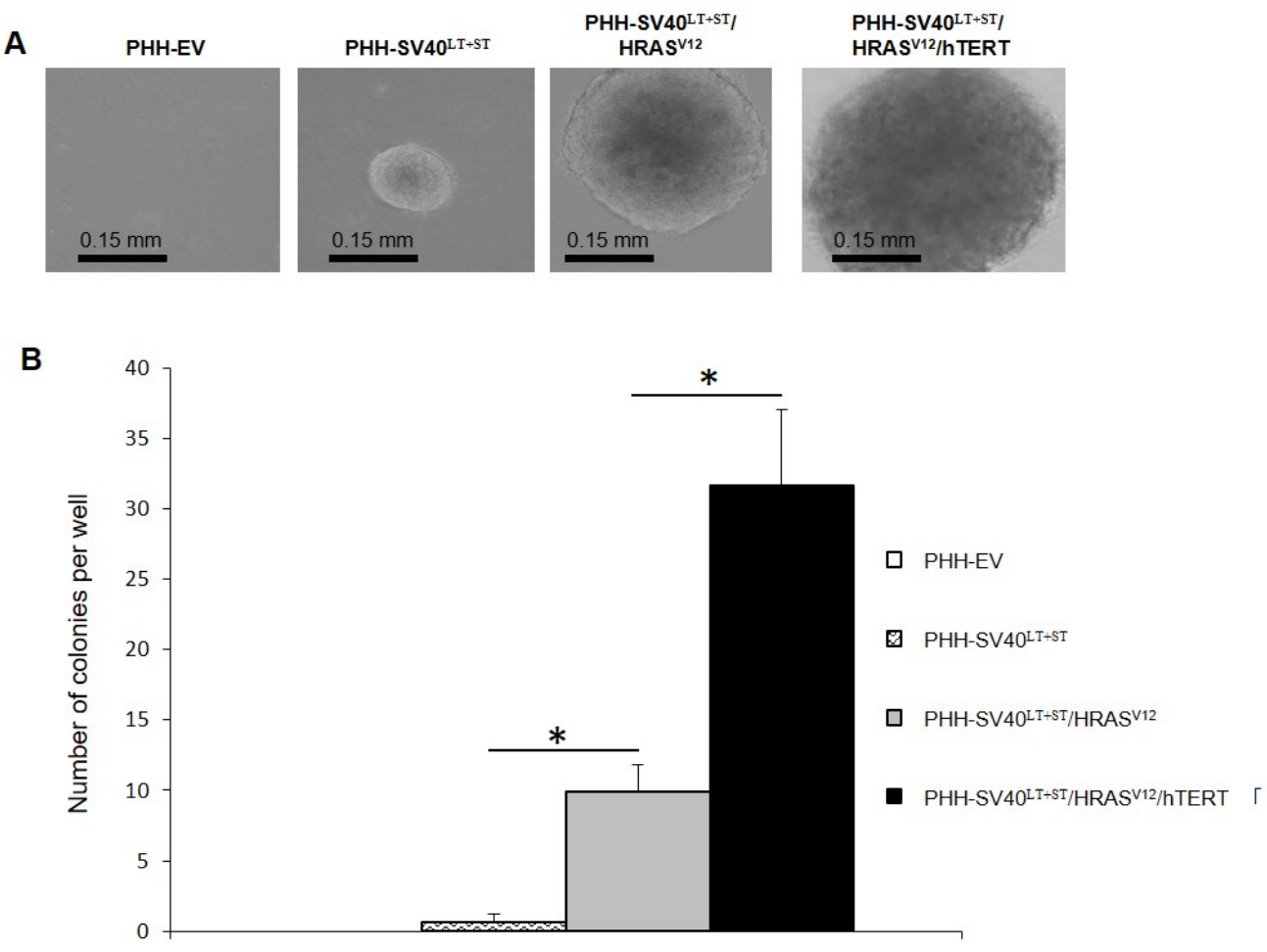
A
PHH-EV
PHH-SV40LT+ST
PHH-SV40LT+ST/ HRASV12
PHH-SV40LT+ST/ HRASV12/hTERT
0.15 mm
0.15 mm
0.15 mm
0.15 mm
B
Number of colonies per well
0
5
10
15
20
25
30
35
40
*
*
PHH-EV
PHH-SV40LT+ST
PHH-SV40LT+ST/HRASV12
PHH-SV40LT+ST/HRASV12/hTERT

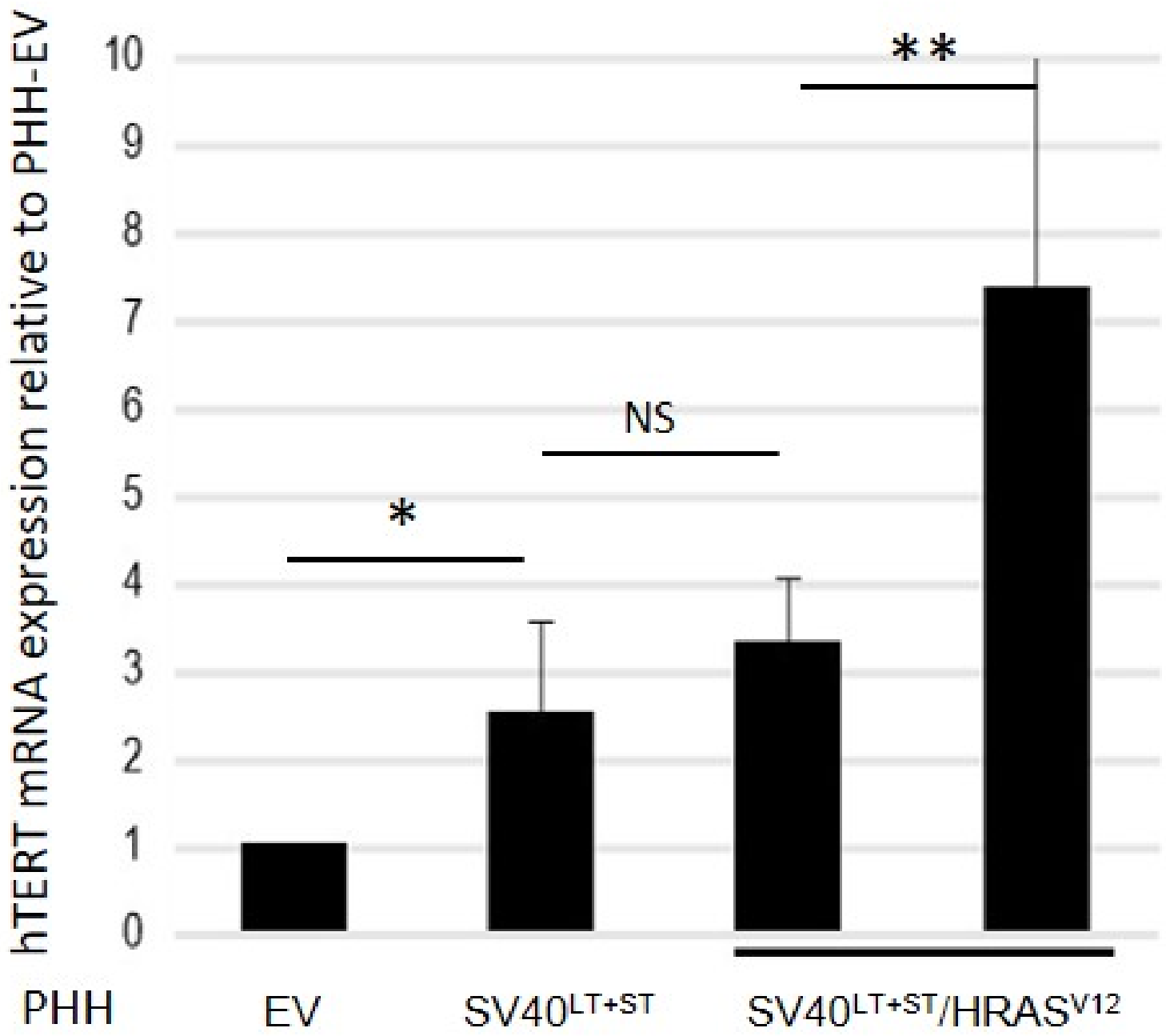
hTERT mRNA expression relative to PHH-EV
10
9
8
7
6
5
4
3
2
1
0
**
NS
*
PHH
EV
SV40LT+ST
SV40LT+ST/HRASV12
Transduced cells in 2D-culture
+
+
+
Agar clones in 2D-culture
+

A

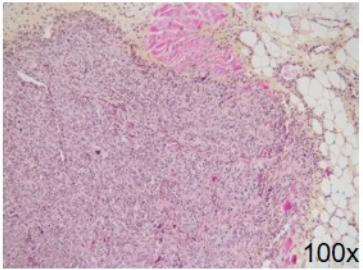
100x

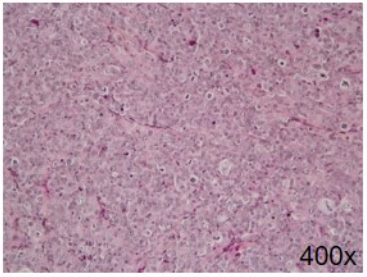
400x

B

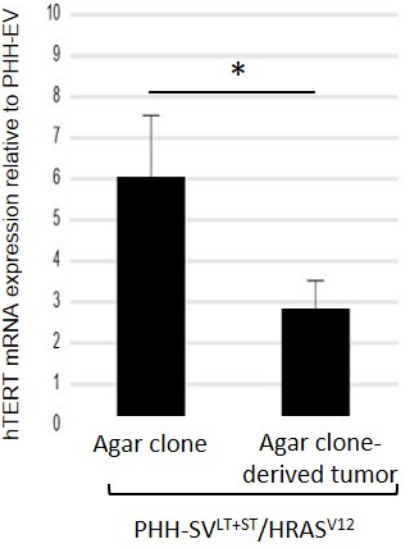
hTERT mRNA expression relative to PHH-EV
10
9
8
7
6
5
4
3
2
1
0
*
Agar clone
Agar clone-derived tumor
PHH-SV^LT+ST/HRAS^V12

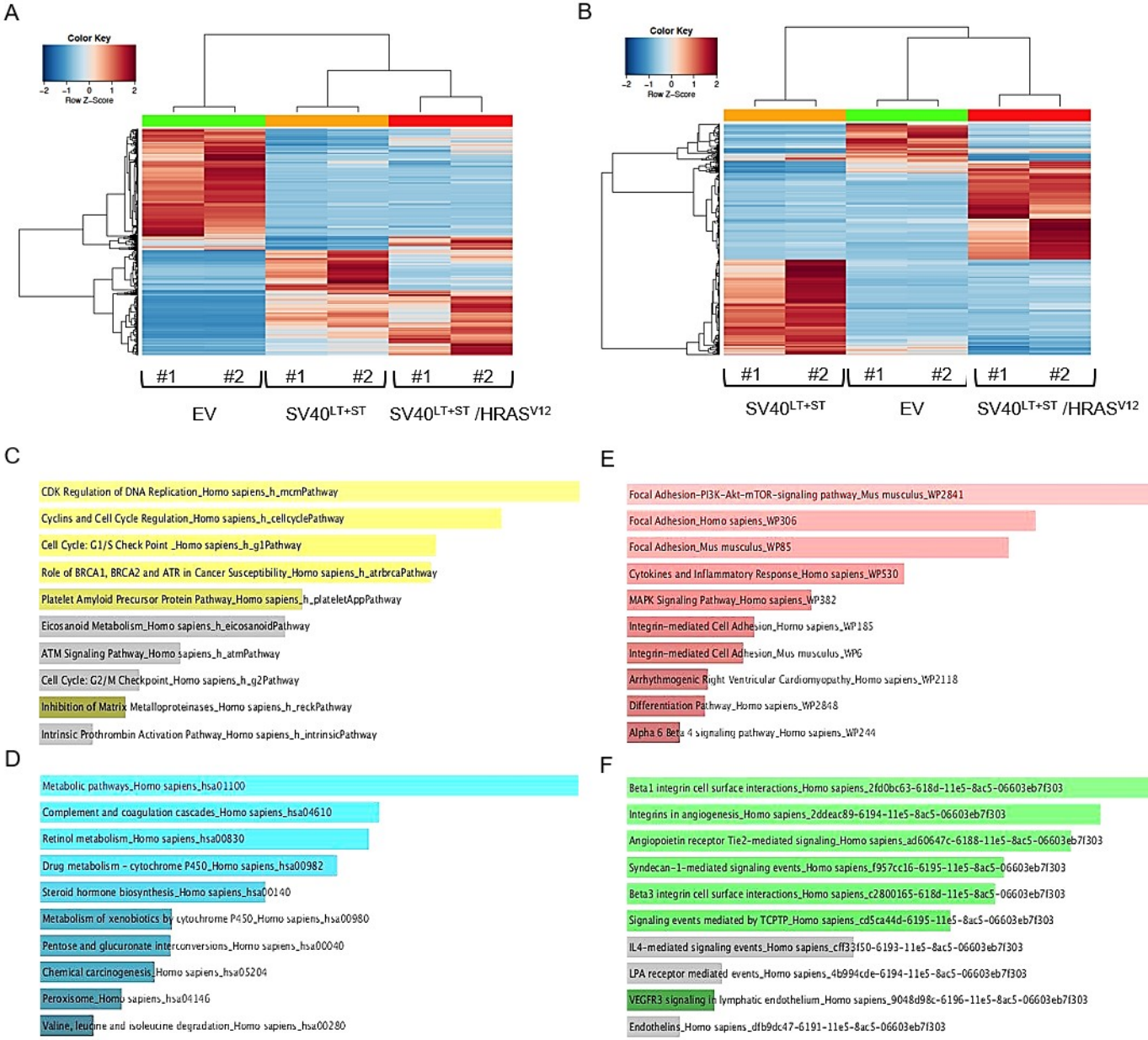
A
Color Key
−2 −1 0 1 2
Row Z-Score
#1 #2 #1 #2 #1 #2
EV
SV40LT+ST
SV40LT+ST /HRASV12
B
Color Key
−2 −1 0 1 2
Row Z-Score
#1 #2 #1 #2 #1 #2
SV40LT+ST
EV
SV40LT+ST /HRASV12
C
CDK Regulation of DNA Replication_Homo sapiens_h_mcmPathway
Cyclins and Cell Cycle Regulation_Homo sapiens_h_cellcyclePathway
Cell Cycle: G1/S Check Point _Homo sapiens_h_g1Pathway
Role of BRCA1, BRCA2 and ATR in Cancer Susceptibility_Homo sapiens_h_atrbrcaPathway
Platelet Amyloid Precursor Protein Pathway_Homo sapiens_h_plateletAppPathway
Eicosanoid Metabolism_Homo sapiens_h_eicosanoidPathway
ATM Signaling Pathway_Homo sapiens_h_atmPathway
Cell Cycle: G2/M Checkpoint_Homo sapiens_h_g2Pathway
Inhibition of Matrix Metalloproteinases_Homo sapiens_h_reckPathway
Intrinsic Prothrombin Activation Pathway_Homo sapiens_h_intrinsicPathway
D
Metabolic pathways_Homo sapiens_hsa01100
Complement and coagulation cascades_Homo sapiens_hsa04610
Retinol metabolism_Homo sapiens_hsa00830
Drug metabolism - cytochrome P450_Homo sapiens_hsa00982
Steroid hormone biosynthesis_Homo sapiens_hsa00140
Metabolism of xenobiotics by cytochrome P450_Homo sapiens_hsa00980
Pentose and glucuronate interconversions_Homo sapiens_hsa00040
Chemical carcinogenesis_Homo sapiens_hsa05204
Peroxisome_Homo sapiens_hsa04146
Valine, leucine and isoleucine degradation_Homo sapiens_hsa00280
E
Focal Adhesion-PI3K-Akt-mTOR-signaling pathway_Mus musculus_WP2841
Focal Adhesion_Homo sapiens_WP306
Focal Adhesion_Mus musculus_WP85
Cytokines and Inflammatory Response_Homo sapiens_WP530
MAPK Signaling Pathway_Homo sapiens_WP382
Integrin-mediated Cell Adhesion_Homo sapiens_WP185
Integrin-mediated Cell Adhesion_Mus musculus_WP6
Arrhythmogenic Right Ventricular Cardiomyopathy_Homo sapiens_WP2118
Differentiation Pathway_Homo sapiens_WP2848
Alpha 6 Beta 4 signaling pathway_Homo sapiens_WP244
F
Beta1 integrin cell surface interactions_Homo sapiens_2fd0bc63-618d-11e5-8ac5-06603eb7f303
Integrins in angiogenesis_Homo sapiens_2ddeac89-6194-11e5-8ac5-06603eb7f303
Angiopoietin receptor Tie2-mediated signaling_Homo sapiens_ad60647c-6188-11e5-8ac5-06603eb7f303
Syndecan-1-mediated signaling events_Homo sapiens_f957cc16-6195-11e5-8ac5-06603eb7f303
Beta3 integrin cell surface interactions_Homo sapiens_c2800165-618d-11e5-8ac5-06603eb7f303
Signaling events mediated by TCPTP_Homo sapiens_cd5ca44d-6195-11e5-8ac5-06603eb7f303
IL4-mediated signaling events_Homo sapiens_cff33f50-6193-11e5-8ac5-06603eb7f303
LPA receptor mediated events_Homo sapiens_4b994cde-6194-11e5-8ac5-06603eb7f303
VEGFR3 signaling in lymphatic endothelium_Homo sapiens_9048d98c-6196-11e5-8ac5-06603eb7f303
Endothelins_Homo sapiens_dfb9dc47-6191-11e5-8ac5-06603eb7f303

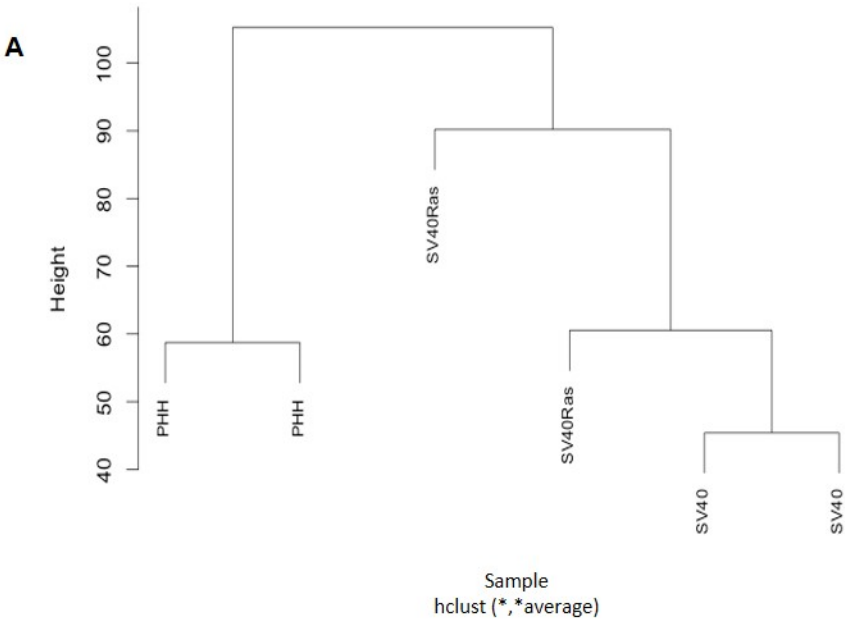
A
Height
100
90
80
70
60
50
40
PHH
PHH
SV40Ras
SV40Ras
SV40
SV40
Sample
hclust (*,*average)

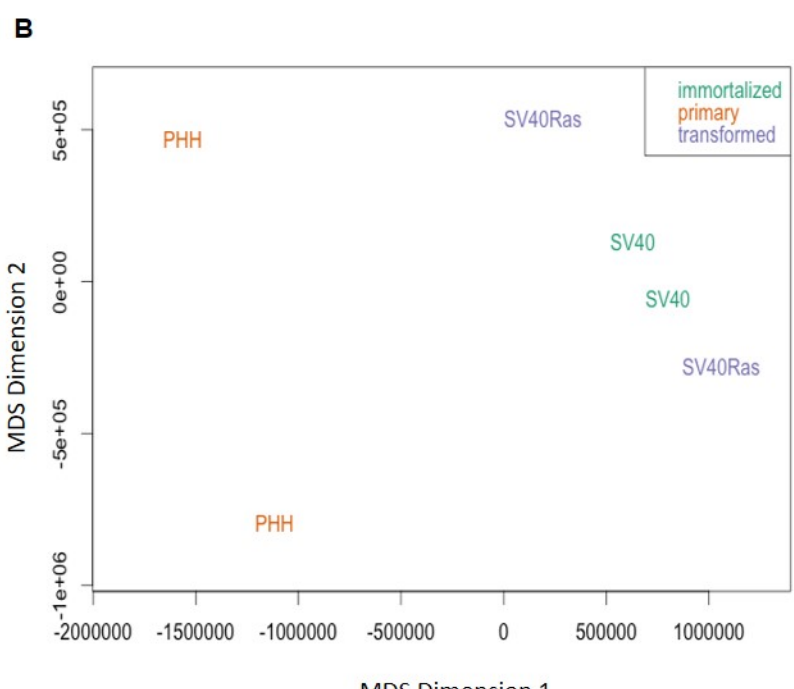
B
immortalized
primary
transformed
PHH
SV40Ras
SV40
SV40
SV40Ras
PHH
MDS Dimension 2
5e+05
0e+00
-5e+05
-1e+06
-2000000
-1500000
-1000000
-500000
0
500000
1000000
MDS Dimension 1

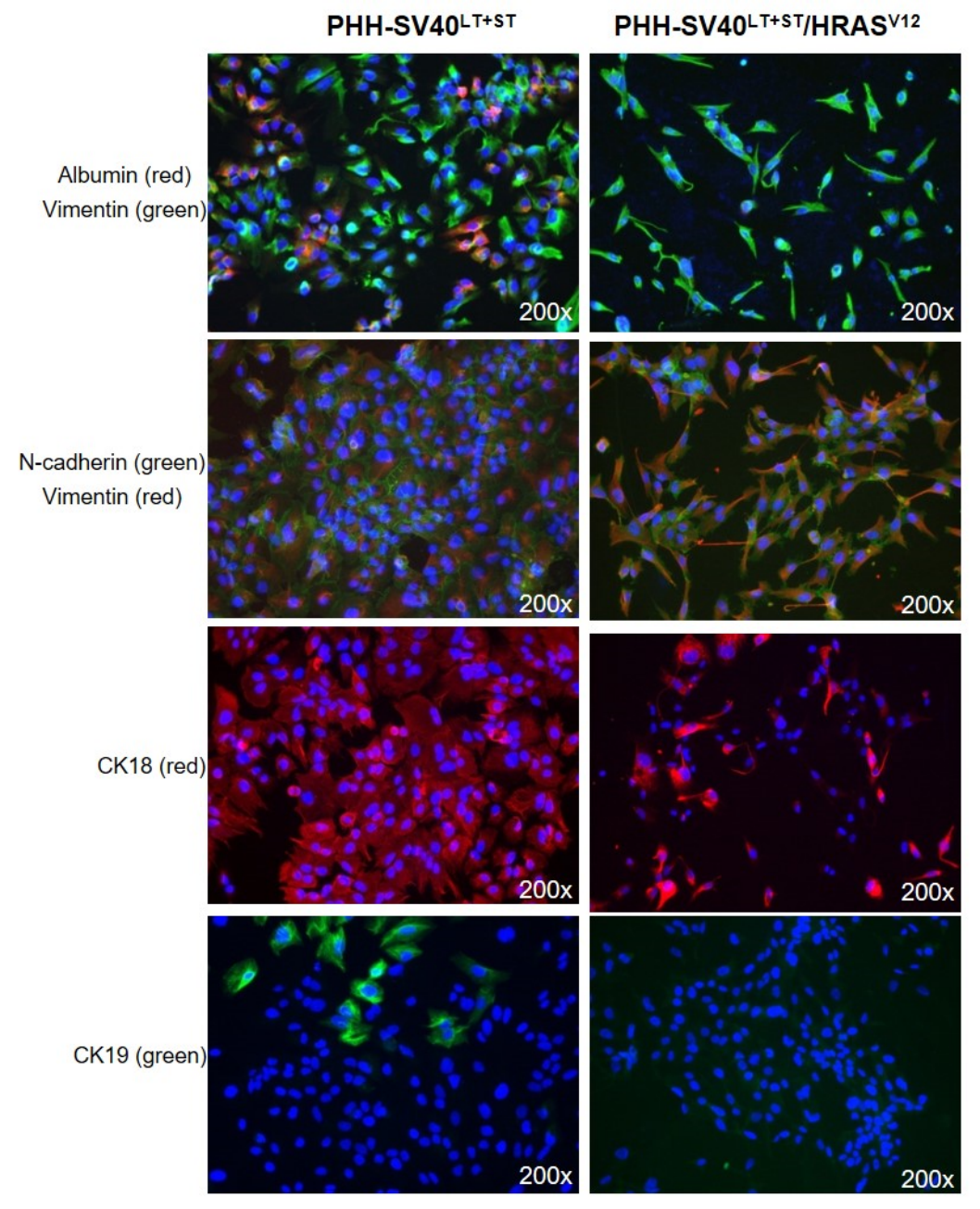
PHH-SV40LT+ST
PHH-SV40LT+ST/HRASV12
Albumin (red)
Vimentin (green)
N-cadherin (green)
Vimentin (red)
CK18 (red)
CK19 (green)
200x
200x
200x
200x
200x
200x

A

PHH-SV40^{LT+ST}

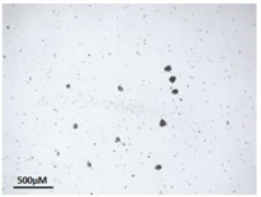

PHH-SV40^{LT+ST}/HRAS^{V12}

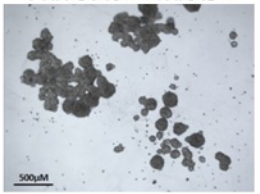

PHH-SV40^{LT+ST}/HRAS^{V12} agar clone

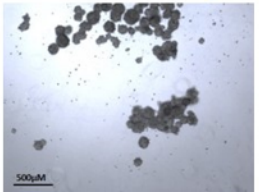

B

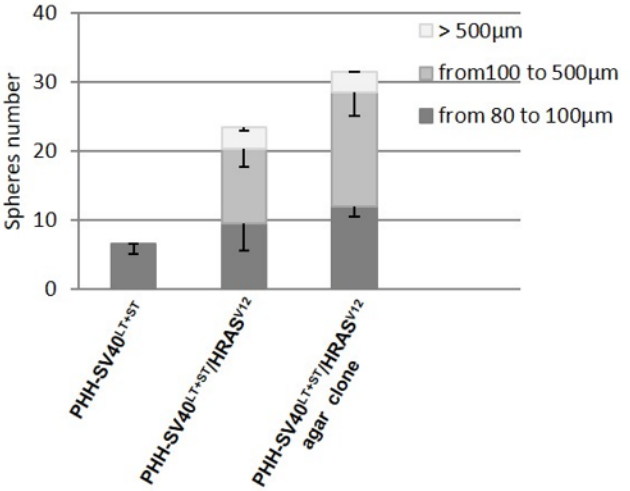

Table 1. Gene expression as assessed by RT-qPCR in PHH-EV, PHH-SV40 and PHH-SV40/HRAS^{V12}. Data were generated from 3 independent experiments, and normalized to PHH-EV.

Gene expression Arbitrary value ± SD	PHH-EV	PHH-SV40	PHH-SV40/HRAS^{V12}
ALBUMIN	1 ± 0.10	$3.7\ 10^{-6} \pm 0.9\ 10^{-6}$	$3.9\ 10^{-5} \pm 0.6\ 10^{-5}$
AAT	1 ± 0.21	0.0002 ± 0.00005	0.0085 ± 0.0003
CYP3A4	1 ± 0.20	0.013 ± 0.003	0.008 ± 0.003
CYP2B6	1 ± 0.26	0.002 ± 0.00005	0.013 ± 0.001
HNF4	1 ± 0.16	0.0003 ± 0.0001	0.0004 ± 0.0002
TAT	1 ± 0.31	0.0002 ± 0.00008	0.0004 ± 0.000001
TDO	1 ± 0.14	0.01 ± 0.0002	0.01 ± 0.0002
CK18	1 ± 0.31	0.24 ± 0.09	0.25 ± 0.02
CK19	1 ± 0.17	6.63 ± 1.18	0.33 ± 0.09
AFP	1 ± 0.26	0.01 ± 0.003	0.009 ± 0.003
DLK1	1 ± 0.34	1.88 ± 0.89	7.32 ± 0.35
EpCAM	1 ± 0.36	0.11 ± 0.02	1.76 ± 0.44
BMI	1 ± 0.29	1.69 ± 0.29	2.15 ± 0.17
NANOG	1 ± 0.31	0.78 ± 0.15	1.98 ± 0.40
OCT4	1 ± 0.60	1.54 ± 0.59	2.21 ± 0.27
SOX2	1 ± 0.22	1.30 ± 1.02	2.53 ± 0.05
FZD7	1 ± 0.60	3.90 ± 0.30	5.40 ± 0.05
ΔNp73	1 ± 0.01	24.0 ± 10.0	18.0 ± 0.05

Table 2. Gene expression as assessed by RT-qPCR in PHH-SV40/HRAS^{V12} tumors developing subcutaneously in nude mice. Data were generated from 3 independent experiments, and normalized to PHH-EV in culture.

Gene expression Arbitrary value ± SD	PHH-EV in culture	Tumors in Nude mice developing from PHH-SV40/HRAS^{V12} cells
ALBUMIN	1 ± 0.03	0.0007 ± 0.0001
AAT	1 ± 0.03	0.004 ± 0.0004
CYP3A4	1 ± 0.07	0.0005 ± 0.00005
CYP2B6	1 ± 0.02	1.31 ± 0.55
HNF4	1 ± 0.05	0.0006 ± 0.00001
TAT	1 ± 0.12	0.00004 ± 0.00002
TDO	1 ± 0.68	0.001 ± 0.00001
CK18	1 ± 0.08	0.57 ± 0.006
CK19	1 ± 0.21	0.01 ± 0.005
hTERT	1 ± 0.29	3.72 ± 0.38

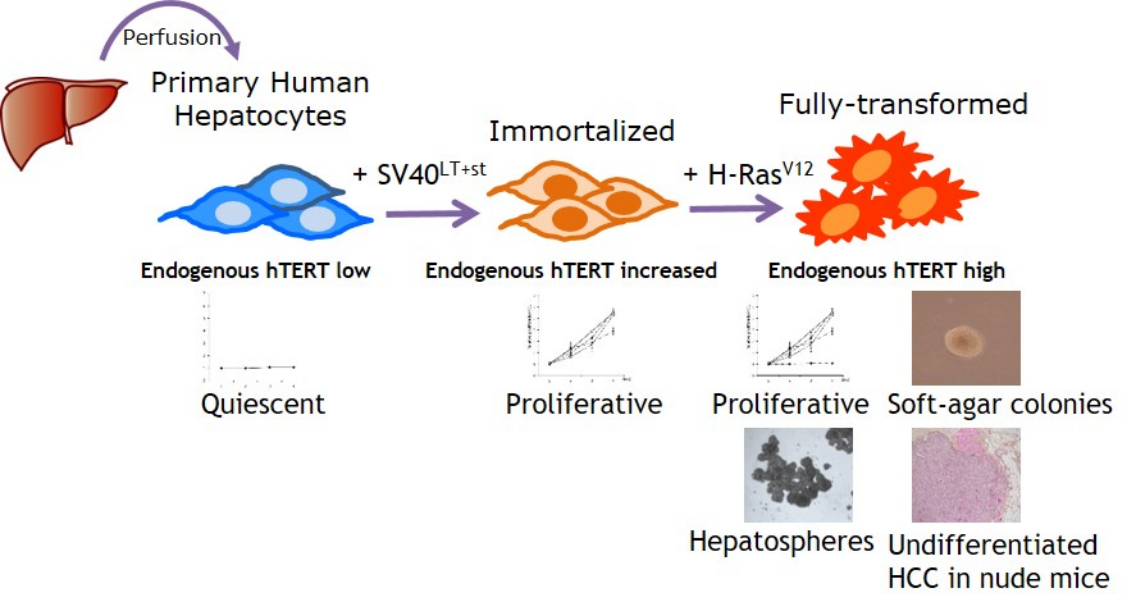
Perfusion
Primary Human Hepatocytes
Immortalized
Fully-transformed
+ SV40LT+st
+ H-RasV12
Endogenous hTERT low
Endogenous hTERT increased
Endogenous hTERT high
Quiescent
Proliferative
Proliferative
Soft-agar colonies
Hepatospheres
Undifferentiated HCC in nude mice